

Small angle X-ray scattering reveals changes of bone mineral habit and size in archaeological bone samples

T. Wess¹, I. Alberts¹, G. Cameron¹, C. Laurie¹, J. Orgel¹, J. Hiller², C. Nielsen Marsh², V. De La Cruz Balthazar³, M. Drakopoulos⁴, A. M. Pollard³, and M. Collins²

[1] Centre for Extracellular Matrix Biology, Dept. of Biological Sciences, University of Stirling, Stirling FK9 4LA, UK.

[2] NRG Unit Fossil Fuels & Env. Geochem. Drummond Building, University of Newcastle-upon-Tyne, UK.

[3] Department of Archaeology, University of Bradford, Bradford, BD7 1DP, UK.

[4] ESRF, Grenoble, 6 rue Jules Horowitz, 38043Grenoble, France.

X-ray scattering provides a powerful non-destructive technique capable of providing important information about the size, habit and arrangement of mineral crystals in bone. In the case of archaeological bone the changes in the habit of the apatite crystals and recrystallised material may reflect the changes in bone environment that have occurred since death. In the study presented here we have examined a variety of archaeological bones by small-angle X-ray scattering to show the alterations in bone habit that can be adopted after 'diagenetic remodelling'. Furthermore we show that the use of small-angle scattering microfocus technology allows us to probe into the fine structure alterations that can occur in bone as a result of microbial attack and mineral recrystallisation. The integrity of the bone crystallites has a strong correlation with the ability to extract other biomolecules from bone such as osteocalcin and DNA. Alterations in the crystallite habit may explain the success of macromolecule recovery from archaeological samples.

In vivo, bone consists of a matrix of collagen fibrils which provides a framework for calcium hydroxyapatite organisation. The hydroxyapatite is found as discrete needle or plate-like crystal structures with a mean thickness of 25-35 nm (Fratzl et al, 1991). The long term archaeological degeneration of bone involves a number of processes indicating that specific forms of geological or microbial degeneration have occurred (Bell et al, 1996; Nielsen-Marsh et al, 2000). These processes involve the remodelling of the mineral and collagen

matrix of bone. However, the exact nature of the rearrangements is poorly defined. Some processes, such as cooking or cremation, are expected to have a more global effect on crystal habit, whereas bacterial action is expected to produce focal changes in bone character on the micron lengthscale (Hackett, 1981). In order to develop an understanding of properties such as differential diagenetic durability between and within the heterogeneous architecture of bones, it is essential to provide information about changes in crystal habit, orientation and statistical distribution of mean thickness. This will lead to an understanding of the archaeological remodelling that occurs at the molecular level and manifests at the level of macroscopic bone integrity.

Small-angle X-ray diffraction is capable of determining the statistical habit of mineral in tissues such as bone (Fratzl et al, 1996(a)). The technique measures the scattering from the collection of crystals within a bone that are bathed by an X-ray beam. The shape of the scattered X-rays contains two key pieces of information, the invariant and the Porod region. The combination of the two allows parameters such as the average crystal thickness and crystal shape to be determined (Fratzl et al, 1996(a)). This has already proved to be successful in examining the effects of osteoporosis (Fratzl et al, 1994). The technique is less subjective than electron microscopy and also does not rely on factors such as the degree of crystallinity that hampers comparisons made by high angle X-ray diffraction (Ziv and Weiner, 1993).

The development of microfocus techniques (Snigirev and Snigireva, 1995) and highly sensitive X-ray detectors, also allows crystallite texture to be analysed over a micron size range in thin sections of bone where focal changes in mineral habit may have occurred with time. In this study we present data showing the typical shape of X-ray scattering obtained from bones of modern animals and we compare these shapes with the alterations that can take place in both well-preserved and highly remodelled archaeological bones. The use of X-ray microfocus technology allows the textural changes to be exhibited on a μm length-scale and indicates that the local texture of archaeological bone can be highly variable. Macroscopic measurements, such as total organic content and porosity, commonly made on macroscopic samples of archaeological bone, may be obscuring a number of local features which possibly hold the key to differentiation between different

Small angle scattering
profile recorded on
CCD detector

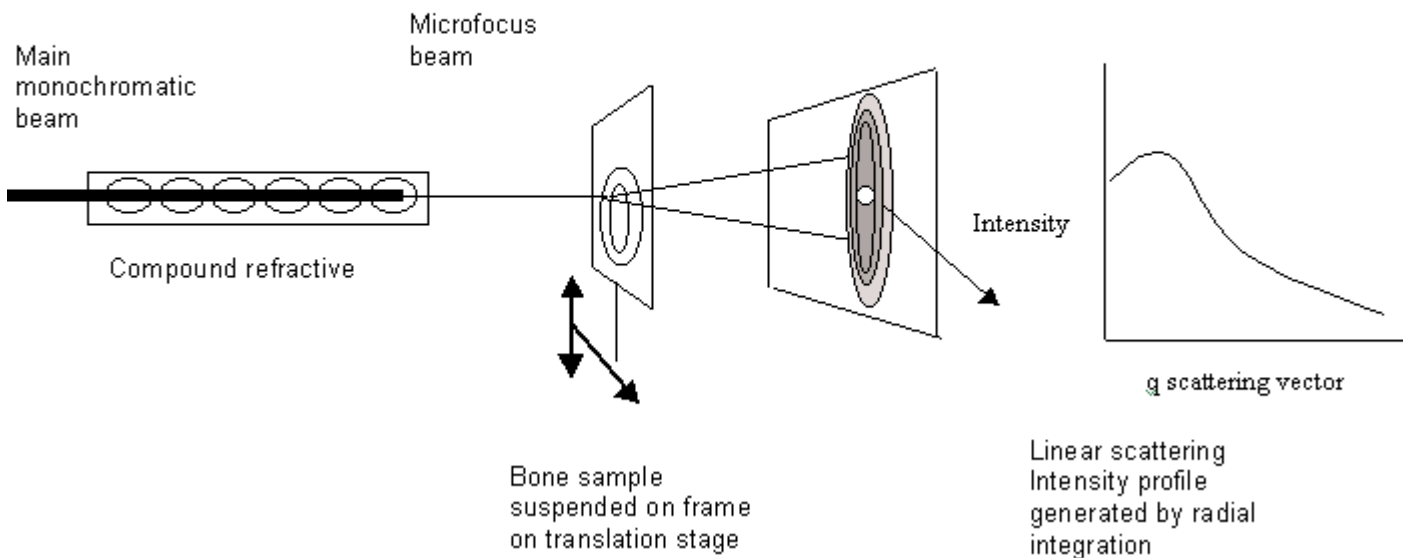


Figure 1: A schematic diagram of the small-angle X-ray scattering geometry for microfocus experiments. The highly parallel monochromatic X-ray beam is defined by an optical element (the compound refractive lens) and used to scan the bone samples. The nature of small-angle diffraction means that the scattered X-rays are close to the main X-ray beam and long camera lengths are used to help resolve the angular scattering components. Data are collected on a CCD detector and then processed as described in the text.

remodelling processes

Materials and Methods

Details of samples and data collection. In this study, 30 archaeological and 10 modern bone samples were analysed. The bones were supplied from the archaeological archives of the Universities of Bradford, Newcastle and Sheffield. The samples exhibited a wide range of deterioration; some bones appeared to be well preserved as judged by microscopic examination of their histology, whereas others were friable and contained no recognisable bone ultrastructural features. Modern bovine femur cortical bone was used as a control sample. The archaeological sample used in microfocus studies was a human femur believed to be aged 1550BP.

All samples were cut on a Leica rotary saw to thicknesses of 50-70 μm , and mounted on mica squares with cyanoacrylate at points where diffraction data were not to be collected. X-ray scattering experiments were conducted at beamline 2.1 of the CCLRC Daresbury synchrotron with complementary microfocus experiments conducted at ID22 of the ESRF Grenoble. At beamline 2.1 at the CCLRC Daresbury synchrotron (Cheshire, UK; Towns-Andrews et al, 1989), a 6m camera length was used to resolve the small-angle scattering profile from the main beam. The spot size at the sample was

500 μm x 2000 μm . The X-ray scattering profile was recorded on a two-dimensional gas filled detector system (for details see Lewis, 1994).

At the ESRF a compound reflective lens (Snigirev et al, 1996) was used to generate a microbeam of size 2 μm vertically by 7 μm horizontally and with a flux of 5.10^9 photons/s, at a wavelength of 0.086 nm. The micro-SAXS patterns were observed with a Fuji photonics low temperature CCD Detector with a recording q range of 0.016 - 4.0 nm^{-1} , where q is the scattering vector $q = 2\pi\sin\theta/\lambda$, θ is the scattering angle and λ the wavelength of incident radiation ($\lambda = 0.086\text{nm}$).

Prior to microfocus scattering, the defocused monochromatic X-ray beam was used to produce an X-ray transmission image of each bone sample. Using the microfocus beam, bones were scanned along a 200 μm -long predefined line at 21 regular intervals that covered regions of what were judged to be intact or modified bone structure. Each individual exposure was in the range of 1-5 seconds. A schematic diagram of the microfocus beamline is shown in Figure 1.

Data treatment The analysis of X-ray small-angle scattering profiles was conducted using the approach of Fratzl et al (1996(a); 1991). Briefly, small-angle

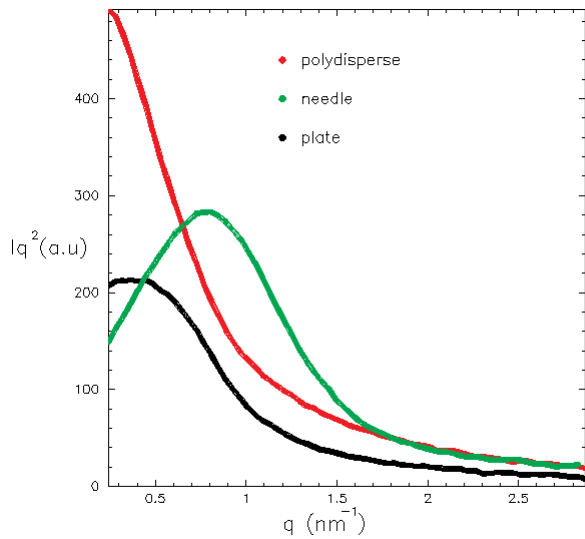


Figure 2: X-ray scattering profiles of bone samples: examples of scattering profiles that show the representative curves corresponding to different crystallite habits. The data are plotted as the intensity multiplied by q^2 where $q = 2\pi\sin\theta/\lambda$ (λ is the wavelength). This is known as a Kratky plot. The profiles shown represent the three main crystalline morphologies that are observed in the bone samples used in this study. The profile marked in red typifies scattering from polydisperse crystal habits. The profile shown in green is typical of needle-like crystals. A third example (scattering profile shown in black) typifies scattering from plate-like crystals.

diffraction profiles were corrected for the dark field current of the detector and were spherically averaged. Two-dimensional images were converted to linear intensity profiles by rebinning data radially in the q range from $0.01 - 3 \text{ nm}^{-1}$. Each profile had an appropriate background profile subtracted, and the resulting linear profiles $I(q)$ converted into Kratky plots ($I(q)q^2$ against q) and Porod plots ($I(q)q^4$ against q^4) that allowed the average crystallite thickness to be defined (see Figure 2).

The scattering profiles indicated that in some cases the habit of the bone varied over the length of the scanned region. This variation was investigated further and quantified. It is preferable to rescale the scattering profiles according to crystal thickness (T) which leads to the definition of a new horizontal axis parameter, $x = qT$. The data were renormalized using the total scattering integrals to give the crystal form factor $G(x)$, such that

Plots of $G(x)$ against x were superimposed and were

used to assess the change in the crystal habit, since they represent the scattering function in relation to the form factor of the crystallite. Quantification of the crystal habit was made by comparing the resultant scattering curve to a Lorentzian curve and calculating the residual η , such that $\eta = [G(x) - G_0(x)]^2 dx$, where G_0 is the normalised Lorentzian function $4 / [\pi(4+x^2)]$. For more detail see Fratzl et al (1996(a)).

Crystal habits such as needles or plates have different characteristic low-angle scattering interactions with X-rays. The size of the crystals also has an effect on the scattering profile. In X-ray scattering, the angular deviation of scatter has an inverse relationship with

size. From this, the position and shape of an X-ray scattering curve can be used to determine the average shape and size of crystallites in a sample.

Multiplying the observed X-ray scattering intensity by the square of the corresponding q value (a parameter derived from the scattering angle) gives a Kratky plot as shown in Figure 2. Needle and plate-like crystals give differently shaped Kratky plots. In the case of plates, the form factor that corresponds to this shape has an intensity profile that decays by a factor of q^{-2} at values close to $q=0$. This leads to a flattened region in the Kratky plot at low q values. In the case of a needle crystal habit, the X-ray scattering form factor of this shape has an intensity that decays in proportion to q^{-1} at low q values, leading to a positive slope at low q in the Kratky plot. Since the plot involves the product of I and q^2 , the differences in the scattering profiles are enhanced and it is relatively easy to distinguish between the two principal crystal types in this study. A further profile that is observed corresponds to a crystal morphology that is neither representative of needle nor plate-like crystals. This scattering curve closely corresponds to a Lorentzian distribution and is thought to correspond to a polydisperse mixture of crystal shapes incorporating large crystal sizes that cannot be studied by small-angle scattering. A thickness measurement, however, can still be made for the part of the crystallite population that is within the domain of small-angle X-ray scattering measurements.

The main parameters that were derived from the study here are the crystal thickness parameter (T) and the shape parameter η . The variation of these

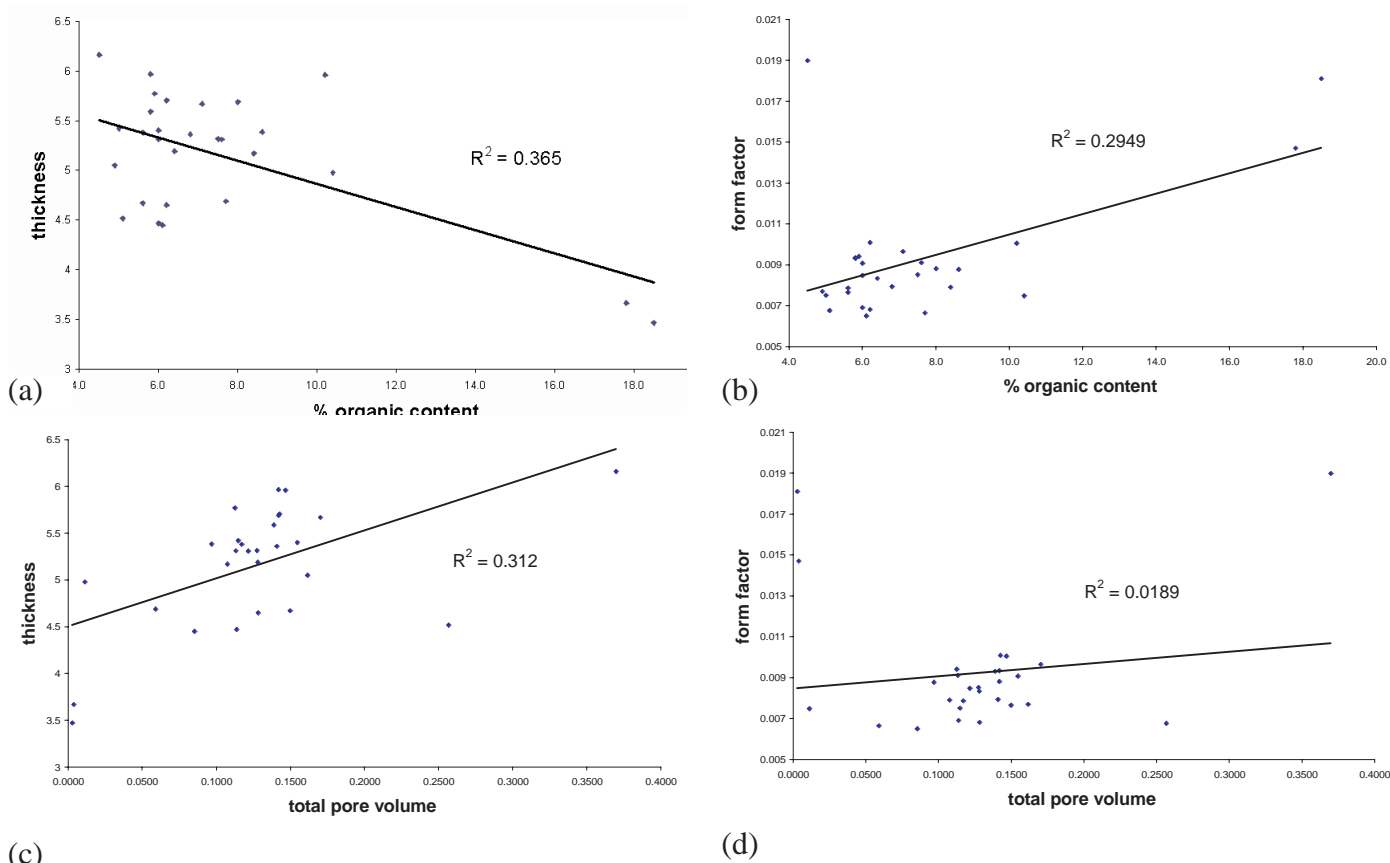


Figure 3: Scatter plot of the thickness parameter T and shape parameter η with allied measurements made on the archaeological sample. Two parameters of interest are the organic content and porosity of archaeological bone. The plots show a line of best fit and a regression analysis value R^2 that is the square of the correlation coefficient. The four scatter plots correspond to:

- (a) the measured organic content against thickness parameter T ;
- (b) the measured organic content against form factor η
- (c) the total pore volume against thickness parameter T and
- (d) the total pore volume against form factor η

The plots contain a number of outlying points. These correspond to the most deteriorated bone which have a negligible organic content and large pore volume. At the other extreme, well preserved bones tend to have a high organic content and low porosity value.

parameters can be assessed between samples using data obtained on a conventional SAXS camera, and can be assessed within an individual sample by analysis of scans made at many points in a sample using microfocus SAXS.

Results

Crystal habit and thickness values from bulk measurements. The bulk measurements of crystallite thickness were derived from the data collected at the Daresbury synchrotron. Here the beam size is 4 orders of magnitude larger than the microfocus line and therefore provides an average of crystallite parameters over a large number of crystallites. It is important that such 'bulk' measurements are made since they are more representative of the size of samples used by archaeologists to obtain

measurements of a number of other parameters such as porosity, total organic content, FTIR signal and histological preservation index. In this study, the major parameters that can be obtained as mean values with standard deviations are the crystal thickness parameter T and the shape function or η parameter.

In comparison to measurements from 10 control modern bones, the average thickness (T) of mineral in archaeological bone (516 nm) is larger than the mean value of control bone (349 nm). The spread of the values given by the coefficient of variation (125 % for archaeological and 120 % for control modern bone) also reveals that a wide range of crystal sizes can be attained by mineral remodelling over time.

The shape parameter is also a quantifiable variable

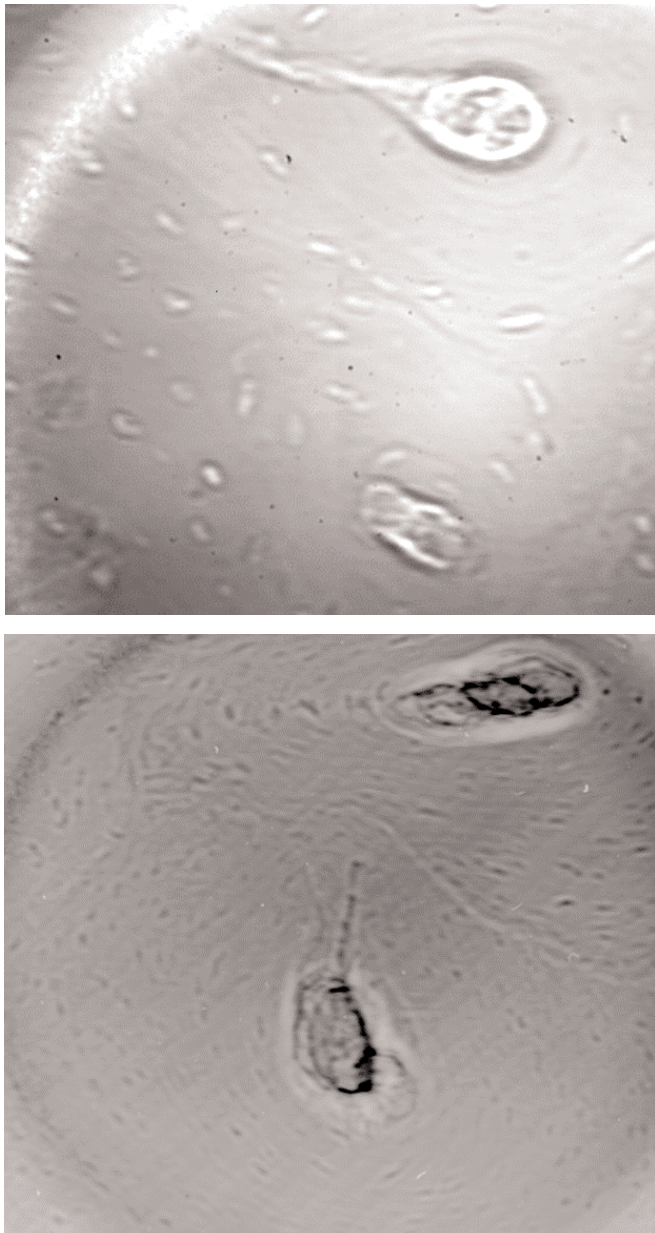


Figure 4: X-ray transmission micrographs of archaeological samples used for microfocus studies: These were obtained by using the unfocused X-ray beam from the ID22 synchrotron beamline at the ESRF, Grenoble. These examples show where scans were performed, as well as the direction of the scan. Each scan is 200 μm in length and 21 measurements were made at equal intervals on each line. The length of a scan also serves as a scale bar. The top image shows a region of cortical bone from a bovine femur and the bottom image is from cortical bone of an archaeological human femur. Both bones show features such as Haversian canals (large ovoids) and osteon lacunae (small ovoids). The deterioration in the archaeological bone is exemplified by the darker regions around the Haversian canal.

that shows the deviation of the scattering profile from the ideal Lorenzian profile. The archaeological bone samples showed a mean shape parameter of 0.009, which suggests that the average shape of the 30 samples is typical of a polydisperse crystal habit. This is not significantly different (according to Student's t-test at the 0.05 significance level) from

the shape profile of modern bones (mean $\eta = 0.011$), which typically give a plate-like crystal habit, although the coefficient of variation is also far greater in the case of archaeological bone (33.3 % versus 90 % for modern bone).

Although it is difficult to make any presumption about the case history of an archaeological bone *post mortem*, it is possible to take representative samples of archaeological bone and to make comparisons of crystal thickness and form factor with other measured parameters. We have chosen to use the total organic content and total pore volume, parameters that may be expected to have a correlation with the bone crystallite thickness. The level of organic material in the bone reflects the collagen content; it could be expected that loss of collagen from archaeological bone removes restrictions on the crystallite shape and size. Furthermore, increased bone porosity may be expected to allow the formation of larger crystallites.

The scatter patterns of these parameters with crystallite size and form factor are shown in Figure 3(A-D). The plots show that there is a moderate correlation between these parameters and crystallite thickness and they allow us to suggest that the effects of porosity and organic content that are on a nm to μm scale reflect the remodelling of crystallites that are at the nanostructural level. The crystal shape parameter shows only a weak correlation with total organic content and no correlation at all with total pore volume, a measure of the porosity of the bone as indicated by nitrogen adsorption. This is probably a consequence of the large variability in η values for the archaeological bones.

Results from microfocus X-ray scattering studies on Archaeological bones. From the results described above, it can be seen that the variability in crystallite shape and thickness between archaeological bone samples is significant. The processes that remodel archaeological bone are thought in part to affect small regions of bone structure and therefore archaeological bone will contain a number of different crystallite textures over relatively small length scales. X-ray microdiffraction of small regions of bone were used to reveal these textural changes. An analysis of a representative microfocus scan is used here to show the capability of the technique.

Images of a thin section of the archaeological and

modern bones used in this study are shown in Figure 4. These were obtained on a high resolution X-ray camera from the transmitted X-ray beam without the microfocus optical elements in place. In both cases the histological features such as the Haversian canal, lacunae and osteons can be seen in cross-section.

The variability of the crystallite habit in the bone samples at various points in each scan line (Figure 4) can be assessed best by comparing the normalised form factor function $G(x)$ for each point in the scan and also by quantifying these parameters by computing η , the shape parameter. This parameter increases with the deviation of scatter from the idealised Lorentzian profile. In this study, polydisperse crystal sizes have low values for η (typically below 0.008), plates have higher values (typically $0.008 < \eta < 0.012$) and needles have values for η typically above 0.012 (corresponding to values derived from Fratzl et al, 1996a), although there is no sharp division between the different shapes.

The $G(x)$ functions, thickness parameter and shape parameter for an archaeological bone sample (Figures 5(a) and 5(b)) are compared to those of a control sample (Figures 5(c) and 5(d)), which corresponds to a typical modern bone. It should be noted that the $G(x)$ functions for all points in the control scan (Figure 5(c)) overlay with very little deviation, and show a very consistent needle-like morphology, which is typical for most modern cortical bones. For the scan in the archaeological bone sample, Figures 5(a) and 5(b) clearly correspond to a local region of bone remodelling, which shows the development of regions of microfocal destruction. This leads to the more variable $G(x)$ functions displayed in Figure 5(a), which indicate a modulation in crystal habit. Examination of the shape parameter as a function of position in the scan (Figure 5(b)), shows that values of η decrease at a specific location between points 10 and 19 of the scan where the nature of the crystallite shape becomes more plate-like. The mineralised bone that surrounds the region of microfocal destruction was judged to be relatively unaltered from a histological perspective and the crystal habit remained as needle type structures.

As shown in Figures 5(b) and (d), the thickness parameter T was rarely larger than 4 nm for either the archaeological or the control bone scans. Changes in crystal thickness were exhibited on two length scales. First, local oscillations of ~ 0.1 nm in the

thickness between consecutive points often occur, corresponding closely to the position of osteons in the sample along the scan. Secondly, undulations of up to 0.5 nm in crystal thickness that occur over a 30-50 μm range. These often correspond to regions of microfocal destruction involving local variation in the shape parameter. This is observed for the archaeological bone scan (Figure 5(d)). As depicted in Figures 5(b) and (d), the variation in the thickness parameter is, in general, significantly less than that of the shape parameter η . For both the archaeological and control bones, the shape parameter and T values along the scans are highly anti-correlated (with correlation coefficients of -0.92 and -0.89, respectively). This indicates a relationship between crystal shape changes and thickness that could provide a basis for remodelling of archaeological bone.

Discussion

Previous studies of crystal habit in bone have shown particular bone classes, such as cortical, lamellar and trabecular bone, to contain what is essentially a consistent crystal morphology; typically needles or plates with relatively little variation over a mm length scale (Fratzl et al, 1996b). X-ray microfocal scattering has the capability of distinguishing the level at which textural variation occurs. This study has demonstrated that local regions of microfocal attack can be identified and the variation in crystal habit statistically analysed using microfocus X-ray technology.

The X-ray microfocus scattering experiments outlined here show the potential for using this technique to map the texture of bone in health, disease, forensic and archaeological contexts.

The ability to extract important structural information at the μm level has shown that local variation within bone texture can be observed and also that data can be represented in a quantified manner. Statistically this clearly has advantages over more subjective microscopical techniques such as scanning and transmission electron microscopy. The observation that the crystal thickness appears to be limited in the samples studied supports the earlier hypothesis of Collins *et al* (1995) that within archaeological bone, regions unaffected by microbial reworking contain essentially intact collagen. The results suggest that the persistence of collagen in bone may regulate the ability of the sample to remodel its mineral *post mortem*, and that the protein

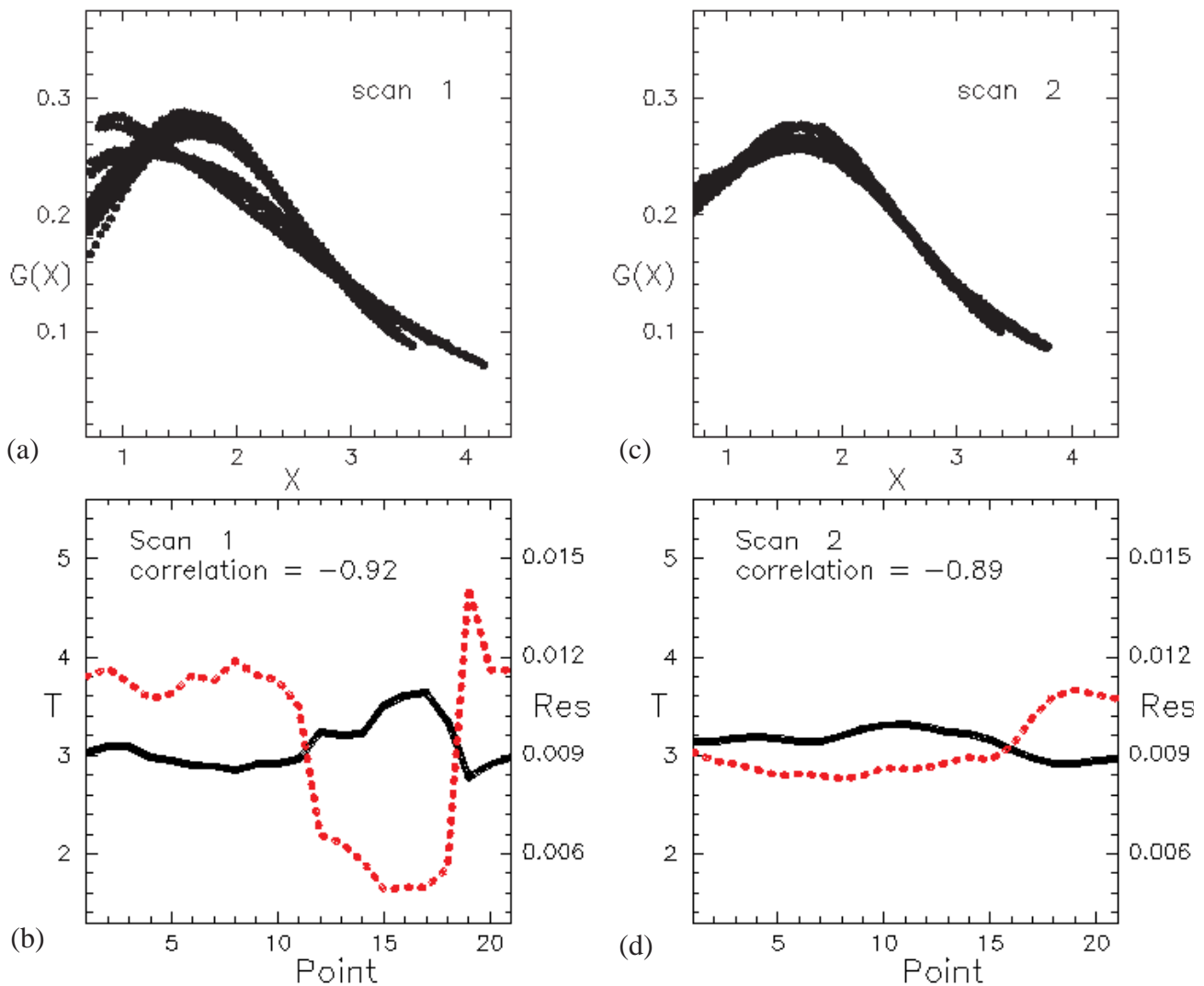


Figure 5: Plots of the crystal form factor $G(x)$ for the scan lines shown in Figure 4 and of the variation of the thickness of the crystallites (T) in comparison with the parameter η . The parameter η shows the deviation of the crystal habit from a Lorentzian distribution as determined by methods described in the text. The variation of the crystal thickness (continuous line) and habit (η dotted line) is shown for a typical control sample of modern human bone and compared to a scan that has been made in regions of an archaeological bone sample.

part of the extracellular matrix is an essential modulator of crystal habit.

The applicability of X-ray scattering studies in general to the field of archaeological bone analysis will allow the deterioration state of bones to be determined in a non-destructive manner. The identical sample can, therefore, also be used for biochemical analysis. Alterations in the crystal habit can be examined in comparison to other effects that are noted in archaeological bone, such as increase in porosity with deterioration (Hedges and Millard, 1995). Bone is a valuable archaeological indicator and significant progress has been made recently in the extraction of DNA from archaeological bone samples. The variability of the amounts and quality of DNA that can be extracted may relate to the alterations of the bone microstructure. Microfocus X-ray scattering is therefore an excellent tool that may be capable of determining the physical basis for the persistence of

bone and its macromolecular contents.

Acknowledgements

We would like to thank all staff at the CCLRC Daresbury synchrotron and ESRF, Grenoble for help in data collection, especially A. Hammersley, A. Snigirev and I. Snigireva. This work was funded by the NERC grant GR 8/5019.

References

- [1] Bell, L.S., Skinner, M.F. & Jones, S.J. (1996) The speed of post mortem change to the human skeleton and its taphonomic significance. *Forensic Science International*, 82, 129-140.
- [2] Collins, M.J., Riley, M.S., Child, A.M. & Turner-Walker, G. (1995) A basic mathematical model for the chemical degradation of ancient collagen. *J. Arch.*

Sci. 22, 175-183.

[3] Fratzl, P., Fratzl-Zelman, N., Klaushofer, K., Vogl, G. & Koller, K. (1991) Nucleation and growth of mineral crystals in bone studied by small-angle X-ray scattering. *Calcif. Tissue Int.* 48, 407-413.

[4] Fratzl, P., Roschger, P., Eschberger, J., Abendroth, B. & Klaushofer, K. (1994) Abnormal bone mineralization after fluoride treatment in osteoporosis: A small-angle x-ray scattering study. *J. Bone Miner. Res.* 9, 1541-1549.

[5] Fratzl, P., Schreiber, S. & Klaushofer, K. (1996a) Bone mineralisation as studied by small-angle scattering. *Connective tissue research* 34, 247-254.

[6] Fratzl, P., Schreiber, S. & Boyde, A. (1996b) Characterization of bone mineral crystals in horse radius by small-angle X-ray scattering. *Calcif. Tissue Int.* 58, 341-346.

[7] Hackett, C.J. (1981) Microscopical focal destruction (tunnels) in exhumed human bones. *Medicine, Science and the Law*, 21:243-264.

[8] Hedges, R.E.M. & Millard, A.R. (1995) Bones and groundwater: towards the modelling of diagenetic processes. *J. Archaeological Science* 22 155-165.

[9] Lewis, R. (1994) Multiwire Gas Proportional Counters: Decrepit Antiques or Classic Performers? *J. Synchrotron Rad.* 1, 43-53

[10] Nielsen-Marsh, C.M., Gernaey, A.M., Turner-Walker, G., Hedges, R.E.M., Pike, A.W.G. & Collins, M. (2000) The chemical degradation of bone in Human Osteology: In 'Archaeology and Forensic Science' (eds Cox, M. and Mays, S.), *Greenwich Medical Media*, London, pp 439-454.

[11] Snigirev, A. & Snigireva, I. (1995) On the possibility of X-ray phase contrast microimaging by coherent high-energy synchrotron radiation. *Rev. Sci. Instrum.* 66, 5486-5490.

[12] Snigirev, A., Kohn, V., Snigireva, I. & Aristova, E. (1996) A compound reflective lens for focussing high energy X-rays. *Nature* 384, 49-51.

[13] Towns-Andrews, E., Berry, A., Bordas, J., Mant, G., Murray, K., Roberts, K., Sumner, I., Worgan, J.S. & Lewis, R. (1989) Time-resolved X-ray diffraction station: X-ray optics, detectors, and data acquisition.

Rev. Sci. Instrum. 60, 2346-2349.

[14] Ziv, V. & Weiner, S. (1993) Bone crystal sizes: a comparison of transmission electron microscopic and X-ray line-width broadening techniques. *Conn. Tissue Res.* 30, 1-14.